AAPS PharmSciTech, Vol. 15, No. 2, April 2014 (© 2014)
DOI: 10.1208/s12249-014-0073-3

Research Article

Dendrimer, Liposomes, Carbon Nanotubes and PLGA Nanoparticles: One Platform Assessment of Drug Delivery Potential

Nishi Mody,[1] Rakesh Kumar Tekade,[1,2] Neelesh Kumar Mehra,[1] Prashant Chopdey,[1] and Narendra Kumar Jain[1,3]

Received 15 September 2013; accepted 23 December 2013; published online 16 January 2014

Abstract. Liposomes (LIP), nanoparticles (NP), dendrimers (DEN), and carbon nanotubes (CNTs), represent eminent classes of drug delivery devices. A study was carried out herewith by employing docetaxel (DTX) as model drug to assess their comparative drug delivery potentials. Under optimized conditions, highest entrapment of DTX was observed in CNT-based formulation (DTX-CNTs, 74.70±4.9%) followed by nanoparticles (DTX-NP, 62.34±1.5%), liposome (49.2±1.51%), and dendrimers (28.26±1.74%). All the formulations were found to be of nanometric size. *In vitro* release studies were carried out in PBS (pH 7.0 and 4.0), wherein all the formulations showed biphasic release pattern. Cytotoxicity assay in human cervical cancer *SiHa* cells inferred lowest IC_{50} value of 1,235.09±41.93 nM with DTX-CNTs, followed by DTX-DEN, DTX-LIP, DTX-NP with IC_{50} values of 1,571.22±151.27, 1,653.98±72.89, 1,922.75±75.15 nM, respectively. Plain DTX showed higher hemolytic toxicity of 22.48±0.94%, however loading of DTX inside nanocarriers drastically reduced its hemolytic toxicity (DTX-DEN, 17.22±0.48%; DTX-LIP, 4.13±0.19%; DTX-NP, 6.43±0.44%; DTX-CNTs, 14.87±1.69%).

KEY WORDS: carbon nanotubes; dendrimer; drug delivery; liposomes; nanoparticles; nanotechnology.

INTRODUCTION

Nanotechnology was well envisioned by Feynman in 1960 and since then gigantic explorations were made by researchers that had made a dramatic impact in all fields of nanotechnology including science and technology (1). Nanotechnology is here with us today and is being used in an evolutionary manner to improve the properties of many therapeutics and health care products (2–4). Concept of nanocarriers was a thought in 1960s and is now taking shape and creating its space in the pharmaceutical market (5–8).

With the advancement in nanotechnology, the integration of nanomaterials into cancer therapeutics is one of the rapidly progressing fields (9,10). Nanocarrier systems can be designed tactically to interact with target cells and tissues or respond to stimuli in well-controlled fashion so as to induce desired physiological responses (11,12). Nanocarriers work by releasing drugs directly into site of action, thereby minimizing the exposure of drugs to healthy tissues. Along with this advantage, enhanced permeability and retention effect (EPR) elicited by nanocarriers further plays a vital role in drug delivery by nanocarriers (13,14). Nanoparticles usually lie in range of 20–200 nm whereas endothelial pores vary within the range of 10–1,000 nm, and hence they can easily extravasate and accumulate inside the tumor interstitial space (15–17).

With present treating regimen for cancer, dose-limited toxicity is a big reason that reduces the efficacy of cancer treatments. In search for more effective cancer treatments, nanosized drug delivery systems, such as liposomes, nanoparticles, dendrimers, and carbon nanotubes that are capable of delivering their drug payload selectively to cancer cells are among the most promising approaches. Liposome and nanoparticles are the two highly investigated moieties in recent years while dendrimers and carbon nanotubes are seeking much attention nowadays for biomedical applications including the field of oncology.

Over the last two decades, a large number of nanocarriers have been developed for cancer therapy and many of them are in the preclinical and clinical stages. These systems are part of the state of the art in the clinics, and an even greater number of nanoparticle platforms are currently in the preclinical stages of development. Liposomes are bilayered lipid vesicles which can home both hydrophilic and hydrophobic drugs whereas polymeric nanoparticles are particulate drug delivery systems mainly made up of biocompatible polymers and therefore find vast application in the cancer therapy. Owing to their size, they can deliver drug passively and being composed of phospholipids mainly, they can bypass RES uptake. Their surface can be decorated with different targeting moieties so as to deliver drug to/in the vicinity of affected tissue *via* bioports.

Dendrimers represent a class of three-dimensional monodispersed synthetic macromolecules in which a sequence of layered branches regularly extend from a central core

[1] Pharmaceutics Research Laboratory, Department of Pharmaceutical Sciences, Dr. Hari Singh Gour University, Sagar 470003, MP, India.
[2] Pharmacy Research Station, College of Pharmacy, University of Hawai'i at Hilo, 96720, Hilo, Hawai'i, USA.
[3] To whom correspondence should be addressed. (e-mail: jnarendr@yahoo.co.in; rakeshtekade@gmail.com)

molecule. Due to their precise nanoscale sizes, precise-branched structures, and various surface modifications, dendrimers have been extensively investigated particularly in the therapeutics and diagnosis of cancer.

Carbon nanotubes (CNTs) are needle-like potential carriers of bioactives including drug, genes and proteins. Functionalization of nanotubes render them more soluble, biocompatible, and helps in attaching certain molecules to their surfaces via covalent or non-covalent bonding thereby proving themselves as a good cargo for all levels of targeted therapy in cancer. The needle-like shape of the CNTs enables them to perforate cellular membranes and transport the carried therapeutic molecules to the cellular components (16,17). These nanosystems are continually being explored for curing several diseases, and till date have been evaluated separately for their drug delivery benefits. Every system has its own advantages and contributes, as an individual, for effective treatment of disease. Literature reviewed concludes that so far no comparison has been carried out under the same experimental conditions for assessing their drug delivery aptitude as well as efficiency to deliver the same therapeutic agent. In the present study, we have compared selected nanocarriers (dendrimer, liposomes, carbon nanotubes, Poly (D, L-lactide-co-glycolide) (PLGA) nanoparticles) for their drug delivery potential by comparing them on similar ground of parameters like optimal drug loading efficiency, drug release, hemolytic toxicity, anticancer potential, *etc.* by employing similar anticancer drug (docetaxel, DTX). This study is expected to be of high scientific interest and will help to predict possible fate of hydrophobic loading in these nanocarriers on ground of herewith reported formulation properties.

MATERIALS AND METHODS

Materials

PLGA and DTX were valued gift from M/s Sun Pharma Advanced Research Center (SPARC), Vadodara, India. Soya phosphatidylcholine was liberally gifted by Lipoid, Germany. Cholesterol, Pluronic F-68, and Triton X-100 were purchased from HiMedia, Mumbai, India. Raney Nickel was purchased from Fluka (USA), while ethylene diamine (EDA) and acrylonitrile (ACN) were purchased from Central Drug House (CDH) India. Multi-walled CNTs produced by chemical vapor deposition having carbon content >90%; and diameter×length 10–20 nm×10–30 μm, was purchased from Timesnano, China. Polytetrafluoroethylene (PTFE) filter was purchased from Rankem, India. All other reagents and solvents used were of analytical grade and used without further purification.

Development of Nanocarriers

Preparation of Liposomes (LIP)

Multilamellar liposomal vesicles were prepared by thin film casting method as reported previously (18), with slight modifications. Briefly, phosphatidylcholine (soya PC) and cholesterol (CH) in 7:3 proportions were dissolved in minimum quantity of chloroform/methanol (3:1; *v/v*) in round bottom flask (RBF). A thin film of lipid was casted on the inner surface of the RBF by evaporating the solvent under reduced pressure in a Rotary Flask Evaporator (Superfit, Mumbai, India). The flask was continuously rotated until the film was dried and final traces of solvents were removed under vacuum (Jyoti Scientific Industries, Gwalior, India). The dried lipid film was hydrated with PBS (pH 7.4) to obtain multi lamellar liposomes. Liposomal suspension was further allowed to stand for 3 h in dark at room temperature to attain complete swelling of the vesicles. The resultant suspension was then sonicated in probe sonicator (Soniweld, Mumbai, India) for 1 min to obtain small unilamellar vesicles (SUVs) and characterized.

Preparation of PLGA Nanoparticles (NP)

PLGA nanoparticles were formulated by solvent extraction-evaporation technique with slight modifications (19). Briefly, PLGA was dissolved in ethyl acetate (3% *w/v*) and added to an aqueous phase containing Pluronic F-68 (1% *w/v*) to form an emulsion followed by sonication (Probe Sonicator, Soniweld, Mumbai, India) to form nanoparticles. Emulsion so formed was further stirred for 3 h at room temperature (3,000 rpm) using mechanical stirrer (Remi, Mumbai, India). Prepared nanoparticles were characterized.

Preparation of 5.0G PPI Dendrimer (DEN)

Fifth-generation poly (propylene) imine (5.0G PPI) dendrimer was produced by repeating sequence of reaction steps, in which each additional iterations leads to a higher generation dendrimer, using a reported protocol (20–22). Briefly, ACN was added to aqueous solution of ethylene diamine (EDA) in 5:1 M ratio followed by refluxing the reaction mixture at 80±0.5°C for 1 h to complete the double Michael addition reaction. Un-reacted ACN was removed as a water azeotrope by vacuum distillation (Rotary Flask Evaporator, Superfit, Mumbai, India) at 16 mbar pressure and 40±0.5°C bath temperature to obtain –CN-terminated half-generation. It was further subjected to heterogeneous hydrogenation in a catalytic hydrogenator (Superfit, Mumbai, India) using raney nickel as catalyst. Mixture was hydrogenated at 40 atm pressure and 70±0.5°C temperature for 1 h. The reaction mixture was cooled, filtered and solvent was evaporated under reduced pressure. These reaction sequences yielded yellowish to brownish colored concentrate, which was characterized by IR spectroscopy. The reaction sequences were repeated cyclically upto 5.0G PPI dendrimer. Further, 5.0G PPI was purified by extensive dialysis against double distilled deionized water in a dialysis tubing (MWCO 5 kDa, Sigma, USA) to remove lower generation dendrimers and un-reacted chemicals, and subjected to characterization.

Functionalization of MWCNTs

Functionalization helps in rendering CNTs more biocompatible by increasing their solubility. This was attained in following steps (23).

Hot air oven treatment of MWCNTs. Pristine MWCNTs (500 mg) were kept inside hot air oven (Hot Air Sterilizer, Yorco, New Delhi, India) at 250±0.5°C for 1 h to remove amorphous carbon and metallic impurities present in the sample (24,25).

Carboxylation of MWCNTs. Carboxylation of MWCNTs was performed by the reported method (26–30) with slight modification. Briefly, MWCNTs was treated with the mixture of concentrated H_2SO_4 (98%) and HNO_3 (68%) in 3:1 ratio

for 4 h at 80±0.5°C. The acid-treated MWCNTs was washed several times with double deionized water (200 times dilution) until the pH became neutral, filtered through PTFE filter (Rankem, Mumbai, India) and dried in vacuum oven (Jyoti Scientific Industries, Gwalior, India) (25,27). Carboxylated solid MWCNTs was transferred into a sonication tube containing double deionized water and sonicated for 15 min (Soniweld, Mumbai, India). Carboxylated MWCNTs were thoroughly characterized.

Drug Loading and Formulation Development

Drug Loading and Formulation Development of Liposomes (DTX-LIP)

In liposomes, drug was loaded during the formation of vesicles. Briefly, drug (5 M excess of the total lipid) was dissolved in chloroform: methanol mixture (3:1; *v/v*) along with the previously optimized lipid cholesterol ratio. A thin film of this mixture was casted on the inner surface of the RBF by evaporating the solvent under reduced pressure in a Rotary Flask Evaporator (Superfit, Mumbai, India). The flask was continuously rotated until the film was dried and final traces of solvents were removed under vacuum (Jyoti Scientific Industries, Gwalior, India). The dried lipid film was hydrated with PBS (pH 7.4) to obtain multi lamellar liposomes. Liposomal suspension was further allowed to stand for 3 h in dark at room temperature to attain complete swelling of the vesicles. The percent entrapment efficiency (% EE) was determined by employing Sephadex G-50 column to separate unentrapped drug (31) and determining the drug concentration spectrophotometrically (Cintra 10 GBC UV Visible spectrophotometer, Japan) at λ_{max} 230 nm foillowed by employing the equation:

$$\%\ \text{Entrapment efficiency} = \frac{\text{Amount of total drug taken} - \text{Amount of free drug detected}}{\text{Amount of total drug taken}} \times 100$$

Formulation of Drug Loaded Nanoparticles (DTX-NP)

Drug loading in nanoparticles was carried out following previously reported method (32). Briefly, 2% *w/v* solution of DTX in ethanol was taken along with the polymer in organic phase. Nanoparticles were prepared and percent drug entrapment efficiency was determined using Sephadex G-50 column.

Drug Loading and Formulation Development using 5.0G PPI Dendrimer (DTX-DEN)

DTX was loaded in synthesized 5.0 G PPI dendrimer by equilibrium dialysis method as previously reported (33,34). Briefly, 1:8 M ratio of dendrimer to drug was taken in screw-capped vials and magnetically stirred at 100 rpm (Remi, Mumbai, India) for 48 h. Then the mixture was dialyzed using dialysis bag (MWCO 1-2 KDa,Sigma, India) for 15 min to remove unloaded drug from the formulation, which was estimated spectrophotometrically at λ_{max} 230 nm (Cintra 10 GBC UV Visible spectrophotometer, Japan).

Drug Loading and Formulation Development using MWCNTs (DTX-CNTs)

Briefly, uniformly dispersed (1-min sonication; Soniweld, Mumbai, India) carboxylated MWCNTs were incubated with ethanolic solution of DTX (1:3 ratio *w/w*) for 24 h at room temperature on a magnetic stirrer (Remi, Mumbai, India) at 100 rpm. Unentrapped drug was removed using dialysis tube technique against 25 mL ethanol for 15 min. Entrapment efficiency was determined by UV visible spectrophotometer at λ_{max} 230 nm (Cintra 10 GBC UV Visible spectrophotometer, Japan) (28–30).

Size, Surface Charge, and Entrapment of DTX Loaded Nanocarriers

The particle size and zeta potential of prepared nanoformulations were investigated by dynamic light scattering using a Malvern instrument (Malvern ZS, 90, UK) by dispersion in phosphate buffered saline (PBS) pH 7.4. The zeta potential was assessed by dispersion of prepared nanoformulations in distilled de-ionized sterile water at 25°C. All measurements were recorded in triplicate.

Drug Release Studies

In vitro release profile of entrapped drug from different drug-loaded formulations (DTX-LIP, DTX-NP, DTX-DEN, DTX-CNTs) was studied at pH 4 and 7.4 (PBS (pH 7.4 and 4.0): ethanol (7:3) *v/v*) using dialysis tube diffusion technique (18,32,35). Briefly, drug-loaded formulations were taken into dialysis tubing (MWCO 1–2 kDa, Sigma, India), hermetically sealed from both sides, dipped inside release medium placed on magnetic stirrer (Remi, Mumbai, India) maintained at 37± 0.5°C. Aliquots were withdrawn at definite time points maintaining the strict sink condition by replenishing equivalent amount of fresh solvent. The drug content was determined spectrophotometrically at λ_{max} of 230 nm in UV Visible spectrophotometer (Cintra-10 GBC UV Visible spectrophotometer, Japan).

Hemolytic Toxicity Study

Hemolytic toxicity of all the developed formulations was assessed under similar experimental condition by employing previously reported methodology, with slight modification in procedure (36–38). Briefly, whole human blood was collected

in hiclot anti-vial (HiMedia, Mumbai, India) and centrifuged to collect red blood corpuscles (RBCs). Collected RBCs were suspended in distilled water and normal saline to produce 100% and no hemolysis, respectively. DTX, LIP, NP, DEN, CNTs, DTX-LIP, DTX-NP, DTX-DEN, and DTX-CNTs were added separately to previously labeled test tubes containing mixture of normal saline (4.5 mL) and RBC suspension (1 mL). Quantities were selected in a manner such that the amount of drug was equivalent in all cases. All the samples were incubated at 37±0.5°C for 1 h and centrifuged at 3,000 rpm for 15 min (Remi, Mumbai, India). Supernatant was removed and analyzed spectrophotometrically at λ_{max} 540 nm after appropriate dilution with normal saline (Cintra 10 GBC UV Visible spectrophotometer, Japan). Percent hemolysis was calculated for each sample by considering the absorbance of water as 100% hemolytic sample, employing following equation:

$$\text{Hemolysis}(\%) = \frac{Ab_s - Ab_{S0}}{Ab_{S100} - Ab_{S0}} \times 100$$

where, Ab_s, Ab_{s100}, and Ab_{so} are the absorbances for the sample, control and 0% hemolysis, respectively.

Ex Vivo Cytotoxicity Study

The MTT cytotoxicity assay determines the ability of viable cells to convert a soluble tetrazolium salt [3-(4, 5-dimethylthiazol-2-yl)-2,5-diphenyltetrazolium bromide] (MTT) into an insoluble formazan precipitate (20,37,38). The MTT cytotoxicity assay was performed on human *SiHa* cell lines. The cells were grown in RPMI growth medium (HiMedia, Mumbai, India) supplemented with 10% fetal bovine serum (FBS, Sigma, St Louis, Missouri, USA) and 1% penicillin–streptomycin mixture (Sigma, St Louis, Missouri, USA). The cells growth inhibition activities of samples were evaluated by MTT colorimetric assay. SiHa cells were seeded evenly into 96-well flat-bottomed tissue culture plates (Iwaki Glass, Tokyo, Japan) at 5×10^3 cells/well concentration and incubated for 24 h in a humidified atmosphere of 5% CO_2 at 37±0.5°C. Formulations (DTX-LIP, DTX-NP, DTX-DEN, DTX-CNTs) and plain DTX were added as freshly prepared solutions in concentrations ranging between 100 and 3,200 nM. After predetermined treatment time (48 h), 20 μL of a 5 mg/mL MTT solution in PBS (pH 7.4) was added to each well and the plate was incubated for 2 h at 37±0.5°C, allowing viable cells to reduce the MTT into purple-colored formazan crystals. The formazan crystals were dissolved by addition of 100 μL of Lysin-buffer (10 mM Tris HCl, 75 mM NaCl, 10 mM EDTA, 0.5%*w*/*v* Sodium dodecyl sulphate) containing Proteinase-K (0.15 mg/mL). The absorbance was measured at 570 nm λ_{max} with the help of an ELISA plate reader (Medispec Ins. Ltd, Mumbai, India) at 37±0.5°C. In addition to cytotoxicity pattern, IC_{50} values of all nanoformulations were also determined and compared.

Statistical analysis

Statistical analysis was performed with Graph Pad Instat Software (version 3.0, Graph Pad Software, Inc., San Diego, CA, USA) using one-way ANOVA followed by Tukey–Kramer multiple comparison test. Difference with $P>0.05$ was considered statistically insignificant, whereas $P<0.001$ was considered as extremely significant.

RESULTS

In the current scenario, different nanocarriers like liposomes, nanoparticles, dendrimers, and carbon nanotubes are hot topics of explorations in lab throughout the globe (1,2,4–6,8–11) including our lab (12,20,21,23,25,28–30,34,36–41), and are believed to revolutionize the field of biomedicine. In this line, allied reports on various formulation aspects of these nanocarriers (like size, loading efficacy, release kinetics, hemolytic toxicity, drug delivery potential, tumor localization, *etc.*) are widely available (4–6,8–11,18,20–22,29,30). Since, all these reports are available from investigations performed under different laboratory settings, their comparison seems non-logical. Hence, with this work it was envisaged to compare the formulation aspects as well as drug delivery potential of aforementioned drug delivery carriers of universal interest to generate conclusive data on one platform and under simulated experimental conditions. For this, DTX-loaded liposomes, nanoparticles, dendrimer and carbon nanotubes-based formulations were prepared as reported in literature (18–21,23–27,31,32) and investigated on one platform keeping all experimental conditions constant.

Prepared liposomes and nanoparticles were characterized for their size, size distribution, surface charge and topography. Average vesicle size, size distribution and surface charge were determined in a Zetasizer (Malvern ZS, 90, UK) and topography by TEM analysis. The size of the liposomal vesicles was found to be 185±2.4 nm. Zeta potential of liposomes was found to be –26.9±1.91 mV (Table I; Fig. 1a). The average size of PLGA NPs were found to be 178±1.4 nm (with poly dispersity index (PDI) of 0.235±0.008) The value of the zeta potential was –11.8±0.83 mV (Table I). TEM image of NPs is shown in Fig. 1b.

The 5.0G PPI dendrimer was synthesized by repetition of double Michael addition reaction using EDA as core, and subsequent hydrogenation (reduction) to primary amine terminated generation. Synthesis was confirmed by FTIR spectroscopy (Perkin Elmer 3600 USA) (Fig. 2a). The synthesis was further confirmed by ^{1}H-NMR (Fig. 2b) and TEM analysis (Fig. 1c).

Sidewall modifications provide understanding and control of chemistry or chemical reactivity of MWCNTs (42–45). FTIR spectral analysis was performed on both purified and carboxylated MWCNTs to assess the presence of different functional groups over their surface. The purified MWCNTs depicted less dense peaks at 2,372.2, 1,646.8, and 1,031.9 cm^{-1}respectively (Fig. 3a). Carboxylated MWCNTs depicted few broad strong peaks at 3,420.8, 2,363.4, 1,636.0, 1,287.5, and 1,065.9 cm^{-1} respectively (Fig. 3b). Purified MWCNTs showed slightly negative value of zeta potential (−2.5 mV±0.134) in alkaline condition. The carboxylated MWCNTs shows more negative zeta potential under all tested pH condition.

XRD spectra depict the structural pattern of the purified and carboxylated MWCNTs (Fig. 4a–b). Electron microscopy was also performed to characterize the functionalized nanotubes (Fig. 1d).

Table I. Optimized Formulation Variable and Value of Size, Zeta Potential, and PDI for Liposomes and Nanoparticles

Formulation	Soya PC/ CH ratio	Polymer amount	Stirring speed and time	Sonication time (min)	Average size (nm; ±SD; n=3)	Zeta potential (ζ; mV)	Polydispersity index (PDI)
Liposomes	7:3	–	–	1.0	185±2.4	−26.9±1.91	0.251±0.011
Nanoparticles	–	3% *w/v*	3,000 rpm; 3 h	1.0	178±1.4	−11.8±0.83	0.235±0.008

Particle size and surface charge (zeta potential) was determined in PBS at 25°C by dynamic light scattering using a NICOMP ZLS 380 analyzer (PSS-NICOMP, Santa Barbara, USA)
Results are represented as mean ± SD (n=3)

Drug loading was optimized in all the nanocarrrier formulations (LIP, NP, DEN, and CNTs) so as to load the maximum possible amount of the drug in the systems under similar conditions. Entrapment efficiency was calculated using Sephadex G-50 mini-column in case of liposome and nanoparticles while for 5.0G PPI dendrimer and carboxylated MWCNTs, dialysis tube diffusion technique was used and percent drug entrapped was found to be 49.2±1.5%; 62.34±1.51%; 28.26±1.74%; 74.70±4.92%, repectively, for liposomes, PLGA nanoparticles, 5.0G PPI dendrimers and carboxylated MWCNTs (Fig. 5a).

In vitro release studies of the nano-formulations were carried out in PBS (pH 7.0 and 4.0) to observe the release pattern so that an expected release profile could be generated for the *in vivo* studies. Nano-formulation produced an initial faster release effect wherein DTX release was found to be 27.68±1.34% (DTX-LIP), 23.92±1.06% (DTX-NP), 84.79±1.06% (DTX-DEN), and 32.77±1.14% (DTX-CNTs) of entrapped DTX within 8 h (Fig. 5b). At acidic pH, all the system showed comparatively faster release at the end of eighth hour wherein 37.78±1.15%, 43.95±1.97%, 95.28±1.94%, and 42.67±1.21% drug release, respectively, was observed in case of DTX-LIP, DTX-NP, DTX-DEN, and DTX-CNTs, respectively (Fig. 5c).

Hemolytic toxicity study was performed to monitor the interaction of nanocarrier system with RBCs. Plain DTX showed maximum hemolytic toxicity (22.48±0.94%) due to its toxic nature as well as direct interaction with the RBCs. DTX-loaded carrier systems were found to be less toxic (DTX-LP, DTX-NP, DTX-DEN, and DTX-CNT, 4.13±0.19%, 6.43±0.21%, 17.22±0.48%, and 14.87±0.69%, respectively) as compared to the free drug. Plain MWCNTs (10.46±0.18%) and 5.0G PPI dendrimer (12.26±0.31%) were found to be more toxic to RBCs compared to plain liposomes (0.24±0.01%) and plain nanoparticles (0.32±0.02%). Results of hemolytic toxicity study are shown in Fig. 6.

Cell line-based cytotoxicity experiments (MTT assay) performed on human cervical cancer *SiHa* cell lines clearly suggests a dose-dependent cytotoxicity response by all DTX-based nanoformulations, *i.e.*, decrease in cell survival fraction with increasing concentration (Fig. 7).

The DTX was found to be a potent anticancer analogue with IC_{50} of 1,109.65±145.28 nM. CNTs offered most suitable option for the delivery of DTX with IC_{50} of 1,104.23±41.87 nM, while its deliverance as DTX-DEN, DTX-DEN, and DTX-NP elicited IC_{50} of 1,571.22±137.04, 1,653.98±72.21, and 1,922.75±76.15 nM.

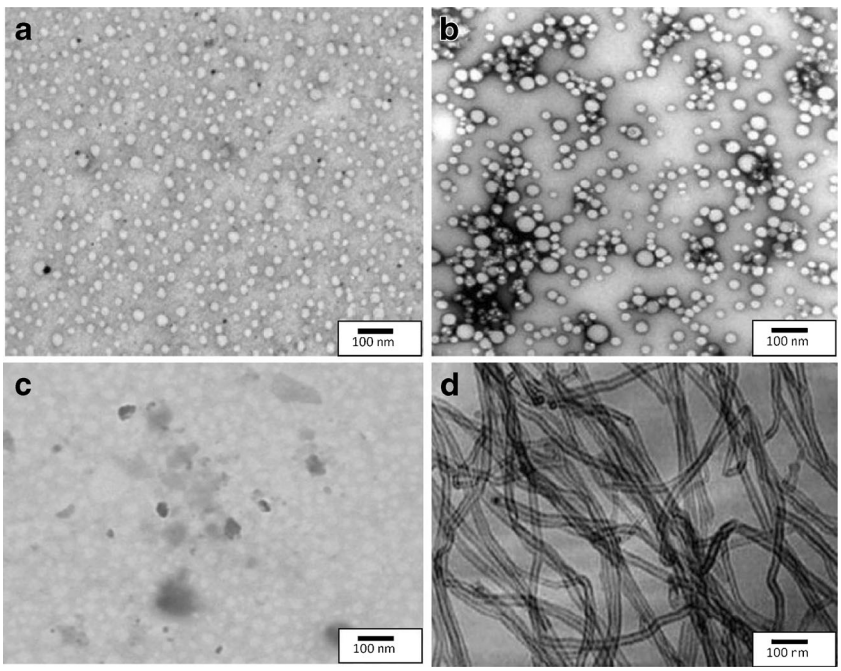

Fig. 1. TEM images of **a** liposomes, **b** PLGA nanoparticles, **c** 5.0G PPI dendrimers, and **d** carboxylated MWCNTs

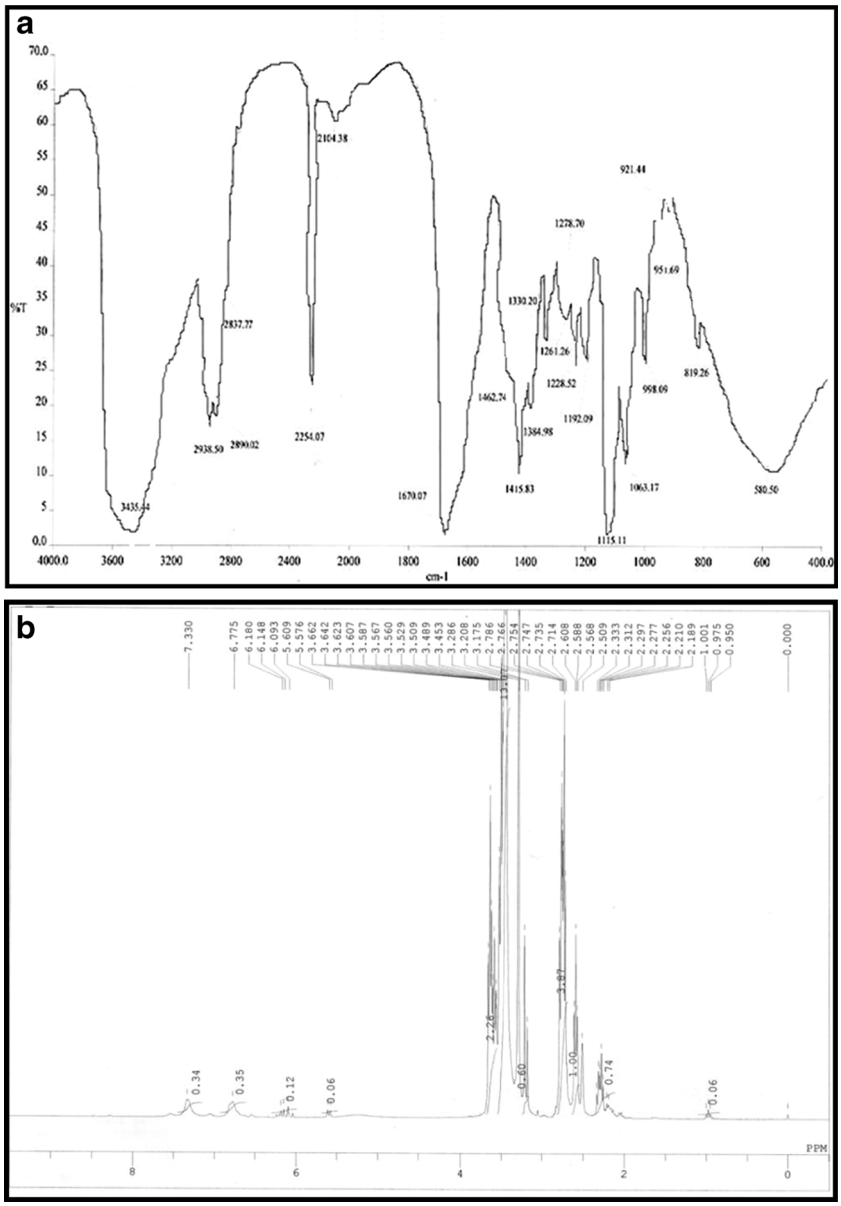

Fig. 2. **a** FTIR and **b** ^{1}H-NMR spectrum of 5.0G PPI dendrimers

DISCUSSION

Liposomal vesicles formed with hand-shaken method were found to be 185±2.4 nm in size making them suitable for passive targeting to the tumor vasculature as these can extravagate and reach the tumor interstitium readily, since tumor vasculature is known to be discontinuous, with gaps ranging from 100 to 780 nm (46). Negative zeta potential of liposomes could be due to the presence of terminal carboxylic groups in the lipid. Electron microscopy revealed that large and small multilamellar vesicles were spherical in shape.

PLGA NPs measured average of 178±1.4 nm with narrow PDI, which places their nomination regarding facilitating the delivery of drug at tumor site *via* EPR effect and make them suitable for effective intracellular uptake. Zeta potential is one of the most important indices to evaluate NP suspension stability. The value of the zeta potential was –11.8±0.83 mV due to the presence of terminal carboxylic groups in the polymer. Electron microscopy image showed that the particles were spherical in shape and do not show considerable variation in shape (Fig. 1b). The results are well in agreement with previous report (47).

EDA was been used as dendrimer core which was confirmed by FTIR spectroscopy (Perkin Elmer 3600 USA) which showed CH_2 rocking (600 cm^{-1}), strong N–H bending vibrations (1,670.07 cm^{-1}), C-H symmetric and asymmetric stretch (2,890.02, 2,938.50 cm^{-1}), very weak peak of C≡N stretch of nitrile (2,254.07 cm^{-1}) indicating the conversion of nitrile into amino terminals and strong N–H stretch of primary amine (3,435.44 cm^{-1}) peaks was obtained that could be attributed to conversion of most of the nitrile terminal dendrimer to amine terminal dendrimer (Fig. 2a). The synthesis was further confirmed by ^{1}H-NMR through obtained major peaks and shifts (Fig. 2b). Peaks of alkane

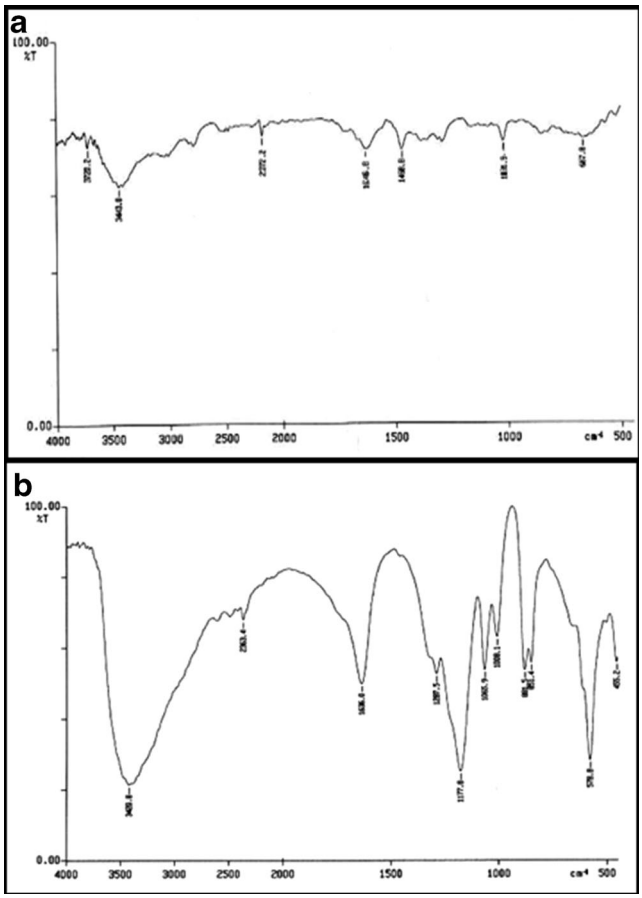

Fig. 3. IR spectrum of **a** purified MWCNTs and **b** carboxylated MWCNTs

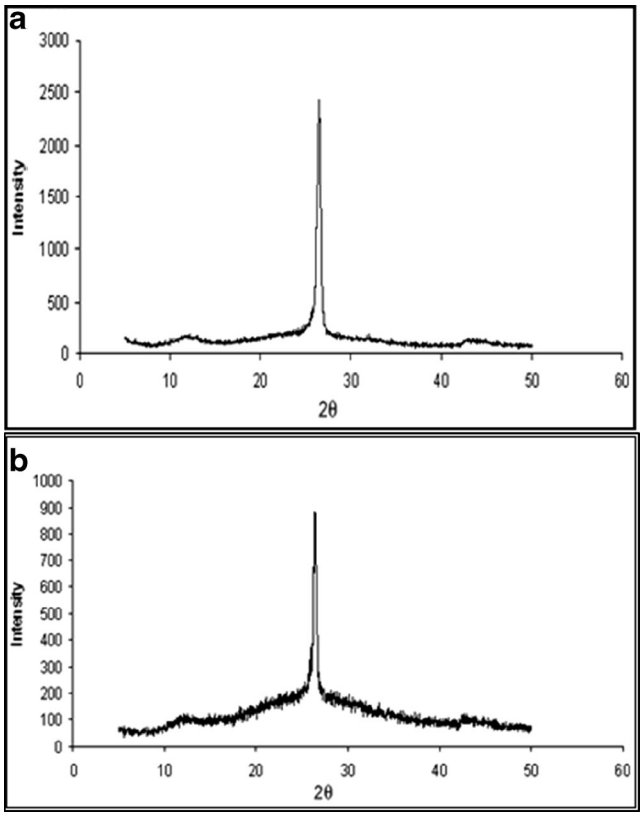

Fig. 4. XRD spectrum of **a** purified MWCNTs and **b** carboxylated MWCNTs

were obtained between 0.12 and .8 ppm while peaks of alkyl amine were obtained between 2.7 and 2.9 ppm. Incompletely cyanoethyleted dendrimer was also evident between 3.2 and 3.6 ppm and primary amines exhibited peak at 7.33 ppm. The electron microscopic analysis of 5.0 G PPI dendrimer proves them to be as nanometric size vesicles as evident by TEM photographs (Fig. 1c). The analytical reports in relation to FTIR and ^{1}H-NMR spectrum showed relevant peaks and the report was in good agreement with previous reports from our laboratory (37–40) (Fig. 2a, b, respectively).

Functionalization and attachment of functional groups to intact MWCNTs proposes various applications in drug delivery aspects, design and characterization of such novel system (48) Purification helps in removing the catalytic and amorphous carbon impurities associated with them. Functionalization and attachment of various functional groups helps in improving the solubility and provide site for tailoring the nanotubes as per need so as to render them more biocompatible and target oriented. The purified MWCNTs depicted less dense peaks at 2,372.2, 1,646.8, and 1,031.9 cm^{-1}, which could be ascribed to the MWCNTs back bone, C–H stretching and O–H in plane bending, respectively (Fig. 3a). These data confirmed the presence of some oxygenated groups generated after purification process. Carboxylated MWCNTs showed few broad strong peaks at 3,420.8, 2,363.4, 1,636.0, 1,287.5, and 1,065.9 cm^{-1}, which could be ascribed to O–H stretching, MWCNT backbone, C=O stretching, C–O stretching and O–H in plane bending, respectively (Fig. 3b). The data confirms the presence of carboxylic (–COOH) groups on the surface of MWCNTs. Negative value of zeta potential (–2.5 mV±0.134) in alkaline condition could be credited to the generation of carboxylic group during purification steps, which usually get ionized in the alkaline pH, thus generating negative value of zeta potential. More negative zeta potential of the carboxylated counterpart under all tested pH condition clearly infers generation of carboxylic group concentration (Table II).

XRD is a technique used to characterize the crystallographic structure, crystal size and preferred orientation in polycrystalline or powdered solid samples (CNTs). Powder diffraction is commonly used to identify unknown substances, by comparing diffraction data against a reference database. XRD spectra depict the structural pattern of the purified and carboxylated MWCNTs and suggest that there is no change in structural integrity of MWCNTs even after undergoing purification steps (treatment with heat/acid) (Fig. 4a–b). The electron microscopic analysis of MWCNTs displayed nanometric size range with tubular structure. The TEM image also suggests control of size and existence of bundles in MWCNTs (Fig. 1d). It was evident from TEM studies that the developed nano carrier systems were of nanometric size range favoring the passive targeting of the loaded drug.

With 5 mol% of drug:lipid ratio, liposomal formulation exhibited highest entrapment (49.2±1.51%; $P<0.01$) (Table III) and <200 nm of size range, which falls within the range required for passive targeting based on EPR effect. Further increase in the amount of drug resulted in decrease in entrapment may be because of the saturation of the lipid layer with the drug. With paclitaxel, Balasubramanian *et al.*,

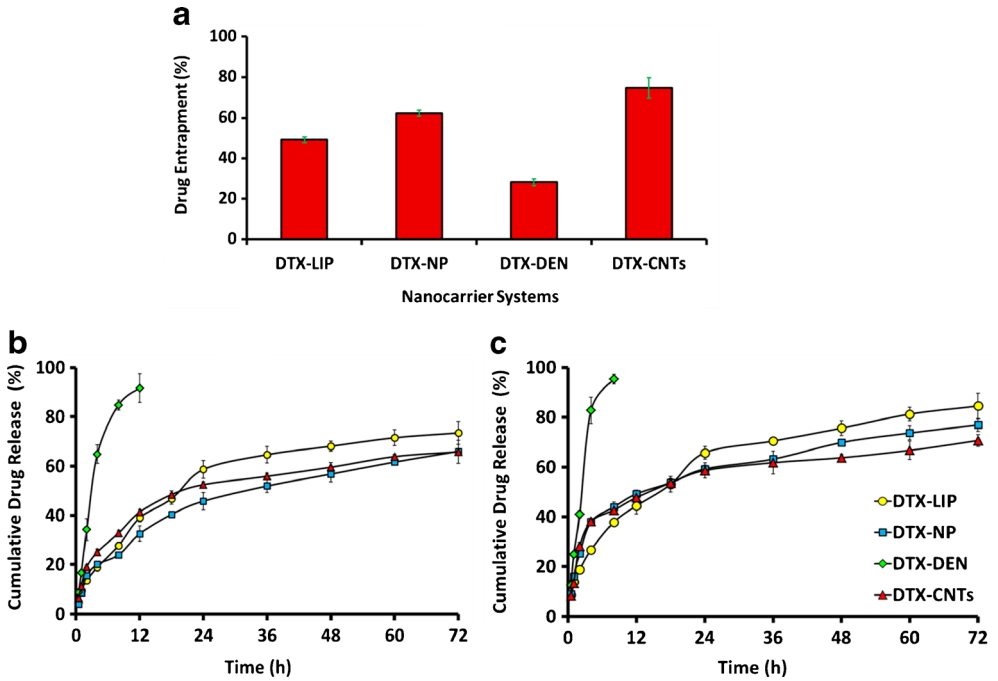

Fig. 5. **a** Comparative percent drug entrapment in selected nanocarriers, **b** cumulative drug release from selected nanocarries at pH 7.4 in PBS (pH 7.4): ethanol(7:3), and **c** at pH 4.0 in PBS(pH 4.0): ethanol(7:3). *DTX*, docetaxel; *DTX-CNTs*, CNT-based DTX formulation; *DTX-NP*, nanoparticles-based DTX formulation; *DTX-DEN*, dendrimer-based DTX formulation; *DTX-LIP*, liposome-based DTX formulation. Results are represented as mean ± SD (n=3)

reported concentration-dependent aggregation in hydrophobic or relatively low polarity environments, forming intermolecular hydrogen bonds. As there is vast structural similarity between paclitaxel and DTX, the later may also show this tendency of concentration dependent aggregation and this might be another possible reason for low entrapment (49). In PLGA nanoparticles, amount of drug loading was optimized on the basis of particle size and percentage entrapment efficiency. It was observed that on increasing the amount of drug, the entrapment efficiency increased up to 2% *w*/*w* (62.34±1.50% P<0.01) of drug while on further increasing the

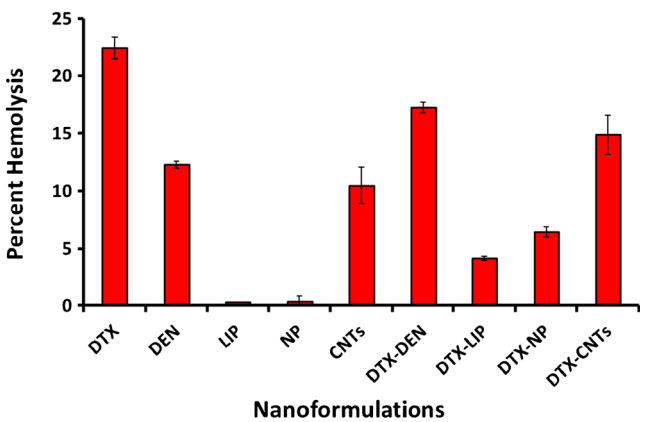

Fig. 6. Percent hemolytic toxicity of nanocarriers under investigation. Keywords: *LIP*, liposomes; *NP*, nanoparticles; *DEN*, dendrimers; *CNTs*, carbon nanotubes (CNTs); *DTX*, docetaxel; *DTX-CNTs*, CNT-based DTX formulation; *DTX-NP*, nanoparticles-based DTX formulation; *DTX-DEN*, dendrimer-based DTX formulation; *DTX-LIP*, liposome-based DTX formulation. Values are represented as mean ± SD (n=3)

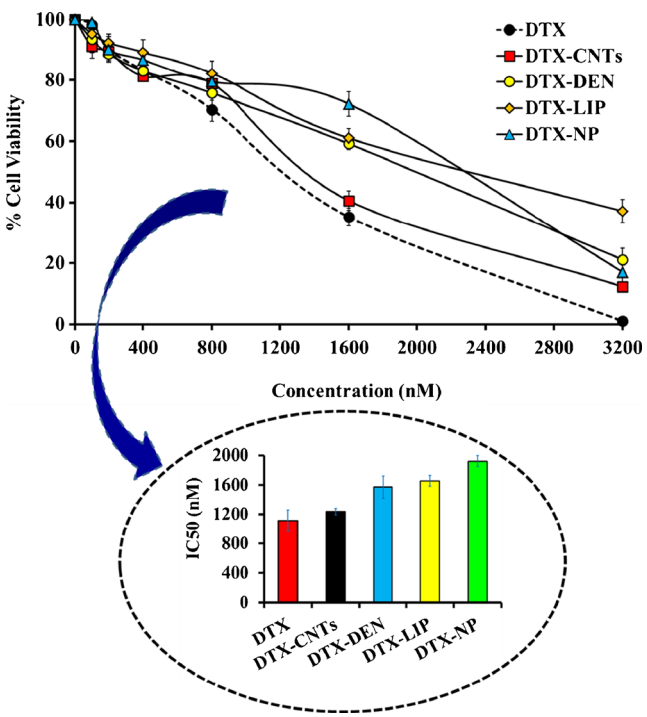

Fig. 7. Cell viability (in percent) after treatment of SiHa cells with different formulations. *Inset* showing IC_{50} value of selected nanocarrier. Keywords: *DTX*, docetaxel; *DTX-CNTs*, CNT-based DTX formulation; *DTX-NP*, nanoparticles-based DTX formulation; *DTX-DEN*, dendrimer-based DTX formulation; *DTX-LIP*, liposome-based DTX formulation. Values are represented as mean ± SD (n=3)

amount of drug, the entrapment efficiency gradually decreased. It could be due to saturation of polymer (PLGA) with the drug (Table III). In case of dendrimer, DTX entrapment takes place within the cavities of the dendritic nanoconstructs (branching clefts) and showed the highest entrapment (28.26±1.74% $P<0.01$) at 1:8 dendrimer: drug ratio On increasing the concentration of the drug to a higher ratio of dendrimer/drug, *i.e.*, more than 1:8, resulted in the saturation of dendritic nano cavities. Thus on further increasing the ratio, decrement in entrapment efficiency was noticed (Table III). With carboxylated MWCNTs, optimization of drug loading was carried out in terms of entrapment efficiency (Table III). Entrapment efficiency of carboxylated MWCNTs was found to be significantly high (74.70±4.92%) than other nanocarriers under investigation (DTX-LIP, 49.2±1.5; DTX-NP, 62.34± 1.51; DTX-DEN, 28.26±1.74) (Fig. 5a) due to the opening of bundles/aggregates and different pores generated by acid treatment. This provides larger surface area and easy penetration into inner cavity of carboxylated MWCNTs. Comparing the entrapment of all four carriers, carboxylated MWCNTs showed the maximum entrapment efficiency due to the high aspect ratio of the nanoconstruct. It provides tubular inner cavities as well as on the surface of the tube wall so the drug moiety can reside inside the tubular structure and also can get appended to the surface with π-π stacking interaction.

All formulations showed biphasic release pattern, initial burst release followed by sustained release profile. The initial burst release may be ascribed to the DTX adsorbed on to the surface of the carrier system. Subsequent to this phase of burst release, a constant drug release profile was observed showing a typical sustained and prolonged release pattern that depends on drug diffusion and matrix erosion mechanisms in case of liposome and nanoparticles. In case of nanotubes, *in vitro* release could also be attributed to the hydrophobic π–π interactions between the graphene of the MWCNTs and phenyl ring of drug molecule that may be responsible for the sustained release of drug. At acidic pH all the system showed comparatively faster release at the end of eighth hour due to the protonation of the groups present on their surface. For instance, carboxylic group in case of liposome, nanoparticles, and carbon nanotubes; and tertiary amines in case of dendrimers are responsible for this protonation resulting in expansion of the nanosystem, which paved the way for faster drug release. Faster release is beneficial for the delivery of anticancer drug as the tumor cells have slightly acidic environment (41).

Hemolytic toxicity study gave a qualitative indication of possible damage to RBC's upon administration of formulations, which is a universal query for all developed formulations. Naked CNTs and 5.0G PPI-DEN were found toxic to erythrocytes with 10.46±1.58% and 12.26±0.31% hemolysis, respectively, due to their charged peripherals. On the other hand, liposome and PLGA-based naked nanocarriers were found to be extremely blood friendly with mere 0.24±0.01% and 0.32±0.01% hemolysis. Liposomes being phospholipidic vesicles are most biocompatible with the biological membranes as phospholipid is the component of the cell wall and hence is non hostile to the erythrocytes. The traces of hemolysis observed might be due to the drug which may be diffused out from the vesicle during the incubation period.

Plain DTX was found to be highly toxic in nature with 22.48±0.94% hemolysis, however loading of DTX inside nanocarrier systems was found to be reducing hemolytic toxicity of DTX as compared to its free form. Higher level of hemolysis was observed with the DTX-DEN and DTX-CNTs formulations as compared to their unloaded counterparts due to transient release of the drug from the carrier system during the incubation period. The hemolytic toxicity of DTX was found to be 4.13±0.19%, 6.43±0.44%, 17.22±0.48%, and 14.87±1.69% in case of its nanoformulation form as DTX-LIP, DTX-NP, DTX-DEN, and DTX-CNTs, respectively. The most significant ($p<0.005$) reduction in hemolytic activity of DTX was observed with liposomal formulation (DTX-LIP, 18.35±1.18% reduction) followed by PLGA nanoparticles

Table III. Optimization of Drug Loading in Various Nanocarriers

Carrier system	Process variable	Average particle size (nm) (mean±S.D. $n=3$)	% Entrapment efficiency (mean±S.D. $n=3$)
Liposomes	Mole % of drug with respect to lipid		
	4	160±2.2	37.5±1.7
	5	179±1.7	38.2±1.9
	6	185±2.4	49.2±1.5
	7	181±1.2	44.72±1.2
Nanoparticles	Drug/polymer ratio (%*w*/*w*)		
	1	170±1.5	28.35±2.7
	2	178±1.4	62.34±1.5
	3	175±1.7	41.45±1.1
	4	182±2.6	35.76±1.3
Dendrimers	Dendrimer/drug ratio		
	1:6	8±0.26	25.54±0.35
	1:7	8±0.39	26.12±0.51
	1:8	8±0.271	28.26±0.74
	1:9	8±0.24	27.34±0.42
	1:10	8±0.12	26.25±0.34
Carbon nanotubes	Carboxylated MWCNTs/drug ratio		
	1:1	210±0.52	54.57±1.1
	1:2	215±0.20	61.54±0.9
	1:3	213±0.19	74.70±1.9
	1:4	212±0.52	71.68±1.3

Results are represented as mean±SD, n=3

Table II. Zeta Potential of MWCNTs

Samples	Zeta potential (ζ; mV)		
	Acidic pH	Neutral pH	Alkaline pH
Purified MWCNTs	+0.5 mV±0.015	+0.45 mV±0.010	−2.5 mV±0.134
Carboxylated MWCNTs	+0.14 mV±0.003	−1.10 mV±0.090	−14.1 mV±0.±0.46

Zeta potential was determined in PBS at 25°C by using a NICOMP ZLS 380 analyzer (PSS-NICOMP, Santa Barbara, USA)
Results are represented as mean ± SD (n=3)

(DTX-NP, 16.05±0.97), CNTs (DTX-CNTs, 7.61% reduction), and dendrimer (DTX-DEN, 5.26±0.63% reduction) (Fig. 6).

MTT assay was executed on *SiHa* cell lines and employing cytotoxicity data, IC_{50} values of all formulations were calculated and represented in Fig. 7. Among all nanoformulations, DTX-CNTs showed lowest IC_{50} value of 1,235.09±0.09 nM in comparison to all other carrier systems under investigation (1,571.22±121.27, 1,653.98±72.89, and 1,922.75±95.15 nM, respectively, for DTX-DEN, DTX-LIP, and DTX-NP, respectively). Highest percentage of viable cells were observed with liposomal formulation indicating minimum cytotoxicity (32.12±1.83%), while free drug was most cytotoxic to the cultured cells as only 01.03±0.92% cell survived after their treatment with the drug alone. Such response could possibly be due to the maximum availability of drug for exerting cytotoxic effect inside the tumor cells. Photomicrograph images of cultured cell treated with different formulations are shown in Fig. 8, which also depicted the maximum apoptosis with DTX-CNTs (Fig. 8f). Finally, it can be concluded that DTX-loaded carboxylated MWCNTs showed better cytotoxicity on cultured

Table IV. Formulation Parameters Observed with Various Nanocarriers: at a Glance

Parameters	Results
Drug entrapment	DTX-CNT>DTX-NP>DTX-LIP>DTX-DEN
Cumulative % drug release (48 h; pH 7.4)	DTX-LIP>DTX-CNTs>DTX-NP>DTX-DEN
Cumulative % drug release (48 h; pH 4.0)	DTX-LIP>DTX-NP>DTX-CNT>DTX-DEN
Hemolytic activity (%)	DTX>DTX-DP>DTX-CNTs>DTX-NP>DTX-LIP
IC_{50} value (SiHa)	DTX-NP>DTX-LIP>DTX-DEN>DTX-CNTs>DTX

Keywords: DTX docetaxel, DTX-CNTs CNT-based DTX formulation, DTX-NP nanoparticles-based DTX formulation, DTX-DEN dendrimer-based DTX formulation, DTX-LIP liposome-based DTX formulation

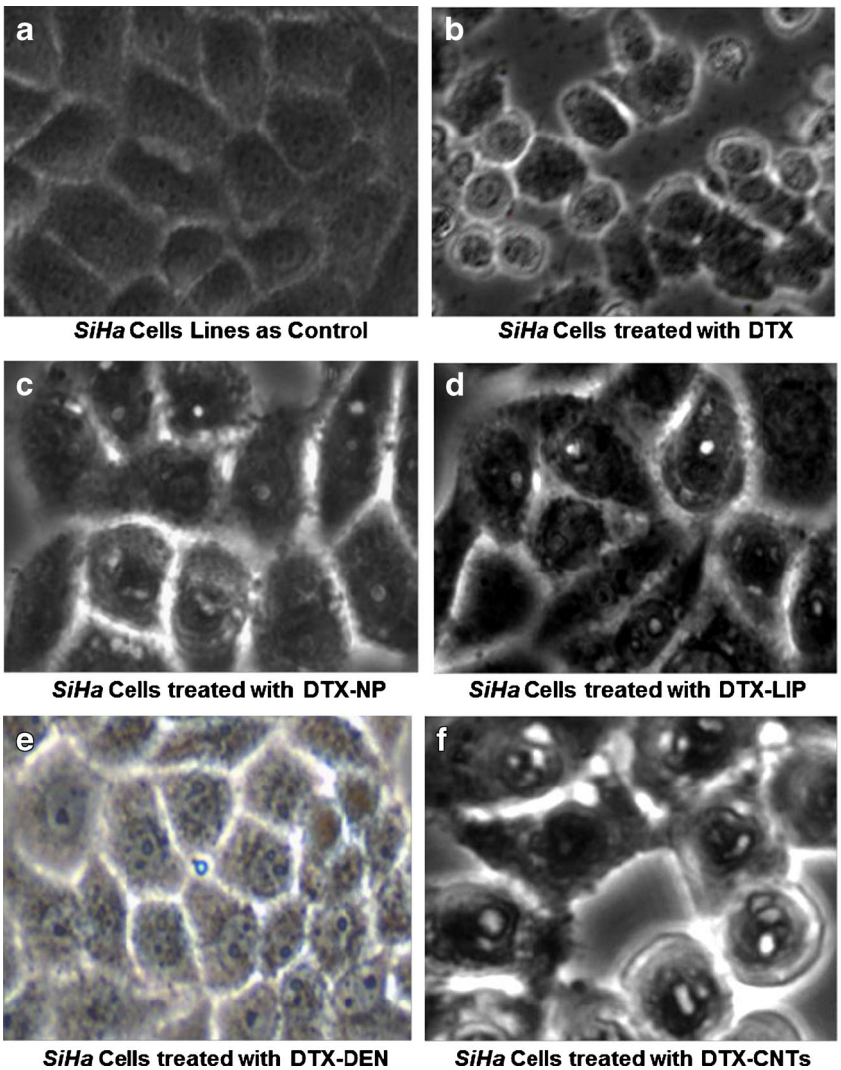

Fig. 8. Photomicrograph of SiHa cell lines (control and formulation treated) indicating apoptosis (×40). Keywords: *DTX*, docetaxel; *DTX-CNTs*, CNT-based DTX formulation; *DTX-NP*, nanoparticles-based DTX formulation; *DTX-DEN*, dendrimer-based DTX formulation; *DTX-LIP*, liposome-based DTX formulation

SiHa cells. CNTs can enter into the cancerous cells by endocytosis mechanism (passive targeting) due to their nano needle tubular structure (50–53). A comparative compilation of drug delivery potentials of various nanocarriers under investigation is conclusively presented in Table IV.

CONCLUSION

Nanotechnology has potentially revolutionized cancer therapy and diagnosis by means of nanocarrier system. In a debut attempt, we have compared four leading nanocarriers (liposomes, PLGA nanoparticles, dendrimer, and carbon nanotubes) for their drug delivery potential employing DTX (anticancer drug) as model bioactive. Developed formulations were characterized and evaluated for their loading efficacy, *in vitro* drug release profile, hemolytic toxicity and cytotoxicity (anticancer benefit). From the outcomes of our studies it can be concluded that in general carboxylated MWCNTs showed better *in vitro*, *ex vivo*, and biocompatibility profile as compared to other carriers under exploration. DTX-CNTs exhibited superior drug release profile especially at acidic pH corresponding to conditions existing at tumorous site. So, carboxylated nanotubes present themselves as potential cargo for anticancer agents and can bring upheaval in the field of cancer therapy but *in vivo* studies shall be essential to have better insight of their toxicological profile (54–57). Although, higher hemolytic toxicity of naked CNTs and dendrimer mandates their surface modification by some appropriate strategy (like PEGylation). Further, it is envisaged that comparative *in vivo* studies and toxicological profiles are additionally warranted for better insight into their therapeutic aspects. An allied investigation comprising of additional leading nanocarrier system are currently under progress in our laboratory.

ACKNOWLEDGEMENTS

The authors would like to thank All India Council of Technical Education (AICTE) and University Grants Commission (UGC), New Delhi (INDIA), for providing the financial assistance. The authors are also grateful to SAIF, Punjab University, Chandigarh, Banaras Hindu University, Varanasi (India), for analytical support, Institute of Cytology and Preventive Oncology, Indian Council of Medical Research, Noida (UP), India, for extending facilities to perform *ex vivo* studies. The authors would also like to acknowledge M/s. Sun Pharma Advanced Research Centre (SPARC) Vadodara, Gujarat, Indi,a for providing the gift samples of DTX and PLGA, and Lipoid, Germany, for generous gift sample of Soya PC.

Conflict of interest No conflict of interest related to this manuscript.

REFERENCES

1. Cho K, Wang X, Nie S, Chen ZG, Shin DM. Therapeutic nanoparticles for drug delivery in cancer. Clin Cancer Res. 2008;14:1310–6.
2. Pal DK, Nayak AK. Nanotechnology for targeted delivery in cancer therapeutics. Int J Pharm Sci Rev Res. 2010;1:1–7.
3. Tomalia DA, Naylor AM, Goddard WA. Starburst dendrimers: molecular-level control of size, shape, surface chemistry, topology, and flexibility from atoms to macroscopic matter. Angew Chem Int Ed. 1990;29:138–75.
4. Solomon R, Gabizon AA. Clinical pharmacology of liposomal anthracyclines: focus on pegylated liposomal doxorubicin. Clin Lymphoma Myeloma. 2008;8:21–32.
5. Bawa R. Nanoparticle based therapeutics in humans: a survey. Nanotech Law Bus. 2008;5:135–55.
6. Fader AN, Rose PG. Abraxane for the treatment of gynecologic cancer patients with severe hypersensitivity reactions to paclitaxel. Int J Gynecol Cancer. 2009;19:1281–3.
7. Danhier F, Feron O, Véronique PV. To exploit the tumor microenvironment: passive and active tumor targeting of nanocarriers for anti-cancer drug delivery. J Control Rel. 2010;148:135–46.
8. Lee KS, Chung HC, Im SA, Park YH, Kim CS, Kim SB, *et al.* Multicenter phase II trial of Genexol-PM, a cremophor-free, polymeric micelle formulation of paclitaxel, in patients with metastatic breast cancer. Breast Cancer Res Treat. 2008;108:241–50.
9. Jiang S, Gnanasammandhan MK, Zhang Y. Optical imaging-guided cancer therapy with fluorescent nanoparticles. J R Soc Interface. 2010;7:3–18.
10. Park JH, Maltzahn GV, Xu MJ, Fogal V, Kotamraju VR, Ruoslathi E, *et al.* Cooperative nanomaterial system to sensitize, target and treat tumors. Proc Natl Acad Sci U S A. 2010;107:981–6.
11. Bharali DJ, Khalil M, Gurbuz M, Simone TM, Mousa SA. Nanoparticles and cancer therapy: a concise review with emphasis on dendrimers. Int J Nanomed. 2009;4:1–7.
12. Tekade RK, Vijayarajkumar P, Jain NK. Dendrimers in oncology: an expanding horizon. Chem Rev. 2009;109:49–87.
13. Li Y, Wang J, Wientjes MG, Au JL. Delivery of nanomedicines to extracellular and intracellular compartments of a solid tumor. Adv Drug Deliv Rev. 2012;64:29–39.
14. Maeda H, Bharate GY, Daruwalla J. Polymeric drugs for efficient tumor targeted drug delivery based on EPR-effect. Euro J Pharm Biopharm. 2009;71:409–19.
15. Panyala NR, Penamendez EM, Havel J. Gold and nano-gold in medicine: overview, toxicology and perspectives. J App Biomed. 2009;7:75–91.
16. Weili Q, Bochu W, Yazhou W, Lichun Y, Yiqiong Z, Pengyu S. Cancer therapy based on nanomaterial and nanocarrier systems. J Nanomat. 2010;1:1–9.
17. Torchilin V. Tumor delivery of macromolecular drugs based on the EPR effect. Adv Drug Del Rev. 2011;63:131–5.
18. Maheshwari RGS, Tekade RK, Sharma PA, Gajanan D, Tyagi A, Patel RP, *et al.* Ethosomes and ultradeformable liposomes for transdermal delivery of clotrimazole: a comparative assessment. Saudi Pharm J. 2012;20:161–70.
19. Song KC, Lee HS, Choung Y, Cho KI, Ahn Y, Choi EJ. The effect of organic phase on the particle size of poly (D, L-lactide-co-glycolide) nanoparticles. Colloid Surf A: Physicochem Eng Aspects. 2006;276:162–7.
20. Tekade RK, Dutta T, Tyagi A, Bharti AC, Das BC, Jain NK. Surface-engineered dendrimers for dual drug delivery: a receptor up-regulation and enhanced cancer targeting strategy. J Drug Target. 2008;16:758–72.
21. Prajapati RN, Tekade RK, Gupta U, Gajbhiye V, Jain NK. Dendimer-mediated solubilization, formulation development and in vitro–in vivo assessment of piroxicam. Mol Pharma. 2009;6:940–50.
22. Agrawal U, Mehra NK, Gupta U, Jain NK. Hyperbranched dendritic nano-carriers for topical delivery of dithranol. J Drug Target. 2013;21:497–506.
23. Mehra NK, Jain AK, Lodhi N, Dubey V, Mishra D, Raj R, *et al.* Challenges in the use of carbon nanotubes in biomedical applications. Crit Rev Ther Drug Carr Syst. 2008;25:169–206.
24. Shen J, Huang W, Wu L, Hu Y, Ye M. Thermo-physical properties of epoxy nanocomposites reinforced with amino-functionalized multi-walled carbon nanotubes. Composites: Part A Applied Sci Manuf. 2007;38:1331–6.
25. Jain AK, Dubey V, Mehra NK, Lodhi N, Nahar M, Mishra DM, *et al.* Carbohydrate-conjugated multiwalled carbon nanotubes: development and characterization. Nanomed: Nanotech Biol Med. 2009;5:432–42.
26. Lin C, Wang Y, Lai Y, Yang W, Jiao F, Zhang H, *et al.* Incorporation of carboxylation multiwalled carbon nanotubes into biodegradable poly (lactic-co-glycolic acid) for bone tissue engineering. ColloSurf B: Biointerfaces. 2011;83:367–75.

27. Li J, Zhang Y. Cutting of multi walled carbon nanotube. App Surf Sci. 2006;252:2944–8.
28. Pruthi J, Mehra NK, Jain NK. Macrophages targeting of amphotericin B through mannosylated multiwalled carbon nanotubes. J Drug Target. 2012;20:593–604.
29. Singh R, Mehra NK, Jain V, Jain NK. Gemcitabine-loaded smart carbon nanotubes for effective targeting to cancer cell. J Drug Target. 2013;21:581–92.
30. Lodhi N, Mehra NK, Jain NK. Development and characterization of dexamethasone mesylate anchored on multi walled carbon nanotubes. J Drug Target. 2013;21:67–76.
31. Fry DW, White JC, Goldman ID. Rapid separation of low molecular weight solutes from liposome without dilution. J Anal Biochem. 1978;90:809–15.
32. Senthilkumar M, Mishra P, Jain NK. Long circulating PEGylated poly (D, L-lactide-co-glycolide) nanoparticulate delivery of DTX to solid tumors. J Drug Target. 2008;16:424–35.
33. Gajbhiye V, Vijayaraj Kumar P, Tekade RK, Jain NK. PEGylated PPI dendritic architectures for sustained delivery of H_2 receptor antagonist. Eur J Med Chem. 2009;44:1155–66.
34. Kumar PV, Asthana A, Dutta T, Jain NK. Intracellular macrophage uptake of rifampicin loaded mannosylated dendrimers. J Drug Target. 2006;14:546–56.
35. Ganesh GNK, Gowthamarajan K, Suresh RK, Senthil V, Jawahar N, Venkatesh N, *et al*. Formulation and evaluation of liposomal drug delivery system for an anticancer drug and the study the effect of various stabilizers based on physicochemical and in-vitro characterization. Int J Pharm Res Develop. 2011;3:27–37.
36. Mishra V, Gupta U, Jain NK. Influence of different generations of poly (propylene imine) dendrimers on human erythrocytes. Pharmazie. 2010;65:891–5.
37. Tekade RK, Dutta T, Gajbhiye V, Jain NK. Exploring dendrimers towards dual–drug delivery: pH responsive simultaneous kinetics. J Microencap. 2009;26:287–96.
38. Kesharwani P, Tekade RK, Gajbhiye V, Jain K, Jain NK. Cancer targeting potential of some ligand-anchored poly (propylene imine) dendrimers: a comparison. Nanomed: Nanotechnol Biol Med. 2011;7:295–304.
39. Bhadra D, Bhadra S, Jain NK. PEGylated lysine based copolymeric dendritic micelles for solubilization and delivery of artemether. J Pharm Pharm Sci. 2005;8:467–82.
40. Gajbhiye V, Vijayaraj Kumar P, Tekade RK, Jain NK. Pharmaceutical and biomedical potential of PEGylated dendrimers. Curr Pharm Design. 2007;13:415–29.
41. Dhakad RS, Tekade RK, Jain NK. Cancer targeting potential of folate targeted nanocarrier under comparative influence of tretinoin and dexamethasone. Curr Drug Deliv. 2013;10:477–91.
42. Ganesh T. Improved biochemical strategies for targeted delivery of taxoids. Bioorg Med Chem. 2007;15:3597–623.
43. Karousis N, Tagmatarchis N. Current progress on the chemical modification of carbon nanotubes. Chem Rev. 2010;110:5366–97.
44. Prato M, Kostas KK, Bianco A. Functionalized carbon nanotubes in drug design and discovery. Acc Chem Res. 2008;41:60–8.
45. Mehra NK, Jain NK. Development, characterization and cancer targeting potential of surface engineered carbon nanotubes. J Drug Target. 2013. doi:10.3109/1061186X.2013.813028.
46. Gupta R, Mehra NK, Jain NK. Fucosylated multiwalled carbon nanotubes for kupffer cells targeting for the treatment of cytokine-induced liver damage. Pharm Research. 2013. doi:10.1007/s11095-013-1162-9.
47. Faranz E, Rassoul D, Hossein MG, Nasser OS, Hadi E, Fatemeh A. Cellular cytotoxicity and in-vivo biodistribution of docetaxel poly (lactide-co glycolide) nanoparticles. Anticancer Drug. 2010;21:43–52.
48. Kuzmany H, Kukovecz A, Simon F, Holzweber M, Kramberger C, Pichler T. Functionalization of carbon nanotubes. Synth Met. 2004;141:113–22.
49. Balasubramanian SV, Alderfer JL, Straubinger RM. Solvent and concentration dependent molecular interactions of taxol (paclitaxel). J Pharm Sci. 1994;83:1470–6.
50. Thakur S, Tekade RK, Jain NK. The effect of polyethylene glycol spacer chain length on the tumor targeting potential of folate modified PPI dendrimers. J. Nanoparticle Res. 2013.
51. Dwivedi P, Tekade RK, Jain NK. Nanoparticulate carrier mediated intranasal delivery of insulin for the restoration of memory signaling in alzheimer's disease. Curr Nanoscience. 2013;9:46–55.
52. Jain NK, Mishra V, Mehra NK. Targeted drug delivery to macrophages. Exp Opin Drug Deliv. 2013;10:353–67.
53. Kam NWS, Dai H. Carbon nanotubes as intracellular protein transporters: generality and biological functionality. J Am Chem Soc. 2005;127:6021–6.
54. Jain NK, Tekade RK. Drug delivery strategies for poorly water–soluble drugs. Kent: Wiley Blackwell; 2012. p. 373–409.
55. Tekade RK, Chougule MB. Formulation development and evaluation of hybrid nanocarrier for cancer therapy: Taguchi orthogonal array based design. Biomed Res Int. 2013. doi:10.1155/2013/712678.
56. Mehra NK, Mishra V, Jain NK. A review of ligand tethered surface engineered carbon nanotubes. Biomat. 2013. doi:10.032/2013.
57. Youngren SR, Tekade RK, Gustilo B, Hoffmann PR, Chougule MB. STAT6 siRNA matrix-loaded gelatin nanocarriers: formulation, characterization, and ex vivo proof of concept using adenocarcinoma cells. Biomed Res Int. 2013;2013:858946. doi:10.1155/2013/858946.